Crystal chemistry of chromian pumpellyite from Osayama, Okayama Prefecture, Japan

MAKI HAMADA,[1,*] MASAHIDE AKASAKA,[1] SHIZUE SETO,[2] AND KUNIAKI MAKINO[3]

[1]Department of Geoscience, Graduate School of Science and Engineering, Shimane University, Matsue 690-8504, Japan
[2]International Technical and Training Center EO Technical Division, EO Training and Application Group,
Jeol Datum Ltd., Akishima, Tokyo 196-0022, Japan
[3]Department of Geology, Faculty of Science, Shinshu University, Asahi 3-1-1, Matsumoto 390-8621, Japan

ABSTRACT

The crystal structure and crystal chemistry of chromian pumpellyite from basic schist in the Osayama ultramafic body, Okayama, Japan, were investigated using electron probe microanalysis (EPMA), Fourier transform infrared spectroscopy (FTIR), and single-crystal X-ray diffraction to determine the distribution of chromium between two independent octahedral sites and structural changes caused by ionic substitutions in pumpellyite, $^{VII}W_8{}^{VI}X_4{}^{VI}Y_8{}^{IV}Z_{12}O_{56-n}(OH)_n$ ($Z = 1$). Five chromian pumpellyite crystals (ocp1211, ocp0604, ocp1028, ocp1013, and ocp1016) with 0.52, 1.65, 1.26, 1.94, and 1.43 Cr atoms per formula unit (apfu) (EPMA data), respectively, were picked from a hand specimen for X-ray diffraction analysis. The crystal structures (space group $C2/m$) of ocp1211 [$a = 19.1129(6)$, $b = 5.8963(5)$, $c = 8.818(1)$ Å, $\beta = 97.449(2)°$], ocp0604 [$a = 19.0935(4)$, $b = 5.900(1)$, $c = 8.810(2)$ Å, $\beta = 97.540(7)°$], ocp1028 [$a = 19.105(2)$, $b = 5.9021(6)$, $c = 8.8143(7)$ Å, $\beta = 97.513(3)°$], ocp1013 [$a = 19.1558(6)$, $b = 5.9125(9)$, $c = 8.844(1)$ Å, $\beta = 97.448(4)°$], and ocp1016 [$a = 19.174(3)$, $b = 5.9194(8)$, $c = 8.830(1)$ Å, $\beta = 97.497(4)°$] were refined using 1058, 829, 1070, 1105, and 1095 unique reflections, and calculations converged at R factors of 4.08, 5.02, 6.32, 6.92, and 7.88%, respectively. The resulting site populations at the X and Y sites are $(Mg_{1.88}Al_{1.51}Fe^{2+}_{0.38}Cr_{0.16}Mn^{2+}_{0.05}Ni_{0.02})^X(Al_{7.90}Ti_{0.07}V_{0.03})^Y$ for ocp1211, $(Mg_{1.81}Al_{1.53}Cr_{0.42}Fe^{2+}_{0.18}Mn^{2+}_{0.04}Ni_{0.01})^X(Al_{7.34}Cr_{0.65}V_{0.01})^Y$ for ocp0604, $(Al_{1.62}Mg_{1.60}Cr_{0.61}Fe^{2+}_{0.13}Mn^{2+}_{0.03}Ni_{0.01})^X(Al_{7.36}Cr_{0.61}V_{0.03})^Y$ for ocp1028, $(Mg_{1.79}Al_{1.33}Cr_{0.47}Fe^{2+}_{0.33}Mn^{2+}_{0.08})^X(Al_{6.66}Cr_{1.31}V_{0.03})^Y$ for ocp1013, and $(Mg_{1.94}Al_{1.23}Cr_{0.38}Fe^{2+}_{0.37}Mn^{2+}_{0.08})^X(Al_{6.72}Cr_{1.25}V_{0.03})^Y$ for ocp1016. Cr^{3+} ions in ocp1211 are distributed only in the X site. The distribution coefficient of Cr and Al between the X and Y sites $[(Cr/Al)^X/(Cr/Al)^Y]$ is 1.66, 1.79, 3.09, and 4.54 for ocp1016, ocp1013, ocp0604, and ocp1028, respectively, indicating a stronger preference of Cr for the X site than the Y site. The a and b axes increase with increasing Cr content, whereas the c axis is almost constant. The mean Y-O distances increase linearly with increased Cr^{3+} content in the Y site. However, the mean X-O distances do not depend on the substitution of Cr^{3+} for Al^{3+} at the X site.

The bond valence sums and the difference-Fourier synthesis indicate that hydroxyl groups are located at the O5, O7, O10, and O11 positions. FTIR spectrum shows main absorption bands at ca. 2911, 3220, 3397, and 3512 cm^{-1} of OH-stretching vibrations, indicating the presence of OH···O hydrogen bonds.

Keywords: Pumpellyite, chromium, X-ray structural analysis, crystal chemistry, FTIR

INTRODUCTION

Pumpellyite, $^{VII}W_8{}^{VI}X_4{}^{VI}Y_8{}^{IV}Z_{12}O_{56-n}(OH)_n$, is an essential rock-forming mineral in low-grade metamorphic and hydrothermally altered rocks. The W and Z sites are essentially occupied by Ca and Si, respectively, the X site by both divalent and trivalent cations, and the Y site by trivalent cations. Pumpellyite-group minerals are named according to the predominant cation in the Y site, where the predominant cation in the X site is denoted by a suffix, following Passaglia and Gottardi (1973). Pumpellyite-group minerals rich in Al^{3+}, Fe^{3+}, Cr^{3+}, Mn^{3+}, and V^{3+} at the Y site have been named pumpellyite (Palache and Vassar 1925), julgoldite (Moore 1971), shuiskite (Ivanov et al. 1981), okhotskite (Togari and Akasaka 1987), and poppiite (Brigatti et al. 2006), respectively. Fe-rich pumpellyites are common in nature, and the

distribution of Fe between the X and Y sites has thus been studied frequently (Allmann and Donnay 1973; Artioli and Geiger 1994; Akasaka et al. 1997; Artioli et al. 2003; Nagashima et al. 2006). Distributions of Mn and V in pumpellyite-group minerals have been examined by Artioli et al. (1996) and Akasaka et al. (1997), and by Brigatti et al. (2006), respectively.

However, despite the approval of shuiskite as a Cr-dominant analog of the pumpellyite group, the distribution of Cr in the two independent X and Y sites remained unknown until the study of Nagashima and Akasaka (2007), who examined chromian pumpellyite from Sarani in the Russian Urals. In that work, they found that Cr^{3+} ions were distributed at both the X and Y sites, preferring the X site over the Y site. Few studies have been made of the crystal chemistry of chromian pumpellyite due to its uncommon natural occurrence (Hamada et al. 2008), and to difficulty in laboratory synthesis.

* E-mail: cr_pumpellyite@yahoo.co.jp

1294

Here we examine the crystal structure and Cr distribution between the octahedral sites in Osayama chromian pumpellyite using single-crystal X-ray diffraction to reveal: (1) distribution of chromium ions among two independent octahedral sites; (2) structural changes caused by the substitution of Cr^{3+} for Al; and (3) crystal chemical rule controlling the distribution of Cr in pumpellyite and structural changes. Presence of hydroxyl groups, as indicated by the X-ray diffraction analysis, was also confirmed using Fourier transform infrared spectroscopy (FTIR).

EXPERIMENTAL METHODS

Specimens

The samples were collected from domains consisting of chromian pumpellyite, chromian phengite, chromian chlorite, and chromite in a basic schist block within the ultramafic body at Osayama, Okayama Prefecture, Japan (Sakamoto 1997; Hamada et al. 2008). Chromian pumpellyite is reddish gray to the naked eye and is colorless in thin sections. It is anhedral in form and exhibits twinning. Grain size varies between 0.05 and 0.3 mm.

For the single-crystal structural analysis of the chromian pumpellyite, chemically homogeneous crystals or grains with high Cr_2O_3 contents in a polished thin section were identified by an electron probe microanalyzer (EPMA) using elemental concentrations maps and quantitative analyses. Three selected chromian pumpellyite grains with dimensions of 0.1 mm × 0.1 mm × 0.1 mm, 0.1 mm × 0.1 mm × 0.1 mm, 0.1 mm × 0.15 mm × 0.05 mm, 0.1 mm × 0.1 mm × 0.05 mm, and 0.05 mm × 0.13 mm × 0.1 mm were then extracted from the thin section [sample 2-3 of Sakamoto (1997); Hamada et al. (2008)] for X-ray intensity data collection. These grains are referred to as ocp1211, ocp0604, ocp1028, ocp1013, and ocp1016, respectively.

Chemical analysis of minerals

The chemical compositions of the chromian pumpellyites were determined using a JEOL JXA-8800M EPMA. Accelerating voltage, specimen current, and beam diameter were 15 kV, 20 nA, and 5 μm, respectively. Natural wollastonite and jadeite (JEOL M3) were employed as standards for Si and Ca and for Na, respectively. Synthetic standards were used for other elements. These were TiO_2 for Ti, spinel for Al and Mg, Cr_2O_3 for Cr, hematite for Fe, $Ca_3V_2O_8$ for V, MnO for Mn, NiO for Ni, $SrBaNb_4O_{12}$ for Sr and Ba, and $KTiO_3$ for K. Monochromators used were TAP for Si$K\alpha$, Al$K\alpha$, Mg$K\alpha$, and Na$K\alpha$; LIF for Ti$K\alpha$, Fe$K\alpha$, Mn$K\alpha$, V$K\alpha$, Cr$K\alpha$, and Ba$L\alpha$; PETH for K$K\alpha$ and Ca$K\alpha$.

Single-crystal X-ray diffraction method

Single-crystal X-ray diffraction data were collected at Shimane University using a RIGAKU R-AXIS RAPID imaging-plate (IP)-mounted two-dimensional X-ray diffractometer system. The chromian pumpellyite crystals were mounted on glass fibers, and intensity data were measured at room temperature using graphite monochromatized Mo$K\alpha$ radiation (λ = 0.71069 Å). Sweeps of data were done using ω scans in 5.0° step for ocp1211 and ocp0604 and in 2.5° for ocp1028, ocp1013, and ocp1016 from 130.0 to 190.0° at χ = 45.0° and φ = 0.0°, and from 0.0 to 160.0° at χ = 45.0° and φ = 180.0°. The data were collected to a maximum θ value at a temperature of 23 °C. The oscillation images collected were total of 44 for ocp1211 and ocp0604, and total of 88 for ocp1028, ocp1013, and ocp1016. Indexing was performed from 5.0° oscillations that were exposed for 180 s for ocp1211 and ocp0604, and from 2.5° oscillations with exposure time of 180 s for ocp1028, ocp1013, and ocp1016. The exposure times for intensity measurement were 300 s/° for ocp1211, ocp1013, and ocp1016, 500 s/° for ocp0604, and 200 s/° for ocp1028. The data were corrected for Lorentz and polarization effects. A symmetry-related empirical absorption was corrected using the ABSCOR program (Higashi 1995).

Unit-cell parameters refined in the scale routine were corrected based on those of two standard materials: cytidine ($C_9H_{13}O_5N_3$) with a = 5.1203(4), b = 13.998(2), c = 14.782(1) Å (RIGAKU); chromian pumpellyite with a = 8.807(6), b = 5.943(4), c = 19.18(1) Å, β = 97.44(2)° (space group $A2/m$) (Nagashima 2006), because of the systematic deviations of the refined unit-cell parameters of the standard materials from their recommended values.

The structure was solved by direct method using the RIGAKU R-AXIS RAPID program with default parameters, and expanded using Fourier techniques. The scattering factors of the neutral atoms (Cromer and Waber 1974) were employed

in our analysis. Anomalous dispersion effects were included in F_{calc}; the values of dispersion corrections for forward scattering used were those of Creagh and McAuley (1992). Values for the mass attenuation coefficients were those of Creagh and Hubbell (1992).

Structural refinement was performed using the SHELXL97 program (Sheldrick 1997). Several refinement cycles were first carried out using the isotropic thermal displacement parameters for the non-hydrogen atoms. Refinement using the anisotropic thermal displacement parameters was then made. Positions of the hydrogen atoms of the hydroxyl groups were derived from difference Fourier synthesis, and were refined assuming full occupancy (occupancy = 1) at a fixed value of the isotropic displacement parameter of U_{iso} = 0.05 Å^2 and with a bond distance constraint of O-H = 0.98 Å (Franks 1973).

FTIR analysis

FTIR microscope spectra of two chromian pumpellyite grains picked up from the thin section of sample 2-3 in the range 1000–4000 cm^{-1} were obtained at Shinshu University, using a Janssen MFT-2000 spectrometer. This range contains absorption bands due to the OH$^-$ stretching vibration. A 50 × 50 μm rectangular aperture was used to obtain suitable spectra. The thickness of the specimens examined was 300 μm, as determined from the focus positions of a microscope (Olympus BX60). The instrumental conditions were: Nichrome source, KRS-5 (TlBr + TlI) polarizer, MCT detector, Ge-containing KBr beamsplitter, instrumental resolution 4.0 cm^{-1}, scan speed 10 mm/s, scan number 32 times and no purge (Nakano et al. 2001).

RESULTS

Chemical compositions of chromian pumpellyite

Chemical compositions of the three Osayama chromian pumpellyite crystals are given in Table 1. Maximum Cr_2O_3 contents of Osayama chromian pumpellyites reach as much as 15 wt% (Sakamoto 1997) and a value of 13.29 wt% has also been reported [Table 2 in Hamada et al. (2008)]. The Cr_2O_3 contents of the five crystals analyzed here are somewhat lower at 2.04, 6.35, 4.87, 7.61, and 5.64 wt%, corresponding to 0.52, 1.65, 1.26, 1.94, and 1.43 atoms per formula unit (apfu), respectively, where the

TABLE 1. Chemical compositions of chromian pumpellyite

	ocp1211	ocp0604	ocp1028	ocp1013	ocp1016
SiO_2	37.85	36.55	38.93	36.67	36.29
TiO_2	0.27	0.04	0.03	0.01	0.00
Al_2O_3	23.91	22.21	20.69	20.96	22.98
Cr_2O_3	2.04	6.35	4.87	7.61	5.64
V_2O_3	0.13	0.05	0.12	0.12	0.11
FeO*	1.40	0.66	0.48	1.22	1.37
MnO	0.20	0.16	0.12	0.28	0.30
NiO	0.09	0.04	0.04	0.04	0.00
MgO	3.92	3.70	3.28	3.72	4.06
CaO	22.39	21.22	22.51	22.64	22.22
BaO	0.15	0.04	0.00	0.00	0.00
K_2O	0.04	0.06	0.06	0.06	0.05
Na_2O	0.21	0.25	0.39	0.21	0.24
Total	92.60	91.33	91.52	93.54	93.26
Cation total = 32					
Si	12.15	12.01	12.76	11.84	11.65
Ti	0.07	0.01	0.01	0.00	0.00
Al	9.04	8.60	7.99	7.98	8.69
Cr^{3+}	0.52	1.65	1.26	1.94	1.43
V^{3+}	0.03	0.01	0.03	0.03	0.03
Fe^{2+}	0.38	0.18	0.13	0.33	0.37
Mn^{2+}	0.05	0.04	0.03	0.08	0.08
Ni	0.02	0.01	0.01	0.01	0.00
Mg	1.88	1.81	1.60	1.79	1.94
Ca	7.70	7.47	7.90	7.83	7.64
Ba	0.02	0.01	0.00	0.00	0.00
K	0.02	0.03	0.03	0.02	0.02
Na	0.13	0.16	0.25	0.13	0.15

* Oxidation state of Fe was determined using the intensity ratio of Fe$L\beta$ and Fe$L\alpha$ lines (Kimura and Akasaka 1999). Under the conditions described, analytical errors are ±2% relative for major elements and ±5% relative for minor elements as estimated from the reproducibility observed in multiple measurements.

total number of cations is 32. The tetrahedral and seven-coordinated sites are essentially filled with Si and Ca, respectively.

FTIR analysis

The spectrum obtained in this study (Fig. 1) is comparable to the vibrational spectra of other pumpellyite-group minerals such as (for example) pumpellyite-(Al) (Hatert et al. 2007). The spectrum shows main absorption bands at ca. 3512, 3397, 3220, and 2911 cm^{-1}. These can be assigned to OH-stretching vibrations. The absorption band around 2230 cm^{-1} is due to CO_2 in the air. The absorption band around 1636 cm^{-1} is typical for the bending vibrations of H_2O (Farmer 1974), but this peak is here assigned to atmospheric H_2O.

Structural solution and refinement

The reflection statistics and systematic absences were consistent with space group $C2/m$. Crystallographic data and refinement parameters are summarized in Table 2. The refined atomic positions are listed in Table 3. The isotropic and aniso-tropic atomic displacement parameters are represented in Tables 3 and 4, respectively. The interatomic distances calculated from the refined atomic positions are shown in Table 5.

By the difference Fourier synthesis, three hydroxyl groups were recognized in ocp1211 (H7, H10, and H11), two in ocp0604 (H5 and H7), ocp1028 (H7 and H11), and one in ocp1016 (H10). In the refinements including the hydrogen atoms for all samples, the $R1$ indices and S-values (goodness-of-fit) converged to the smallest values of 4.08% and 1.088 for ocp1211, 5.02% and 0.954 for ocp0604, 6.32% and 1.039 for ocp1028, 6.92% and 1.564 for ocp1013, and 7.88% and 1.583 for ocp1016 (Table 2).

The site occupancies of Ca at the seven-coordinated W1 and W2 sites, and Si at the tetrahedral Z1, Z2, and Z3 sites were refined at the primary stage of the structural refinement. This revealed that these sites were fully occupied with these respective elements, within their standard deviations. The site occupancies at these sites were thus fixed as 1 Ca at the W1 and W2 sites, and 1 Si at the Z1, Z2, and Z3 sites. The site populations at the X and Y sites listed in Table 6 were determined based on the

TABLE 2. Crystallographic data of the chromian pumpellyite* and experimental details of the single-crystal X-ray diffraction analysis

Sample	ocp1211	ocp0604	ocp1028	ocp1013	ocp1016
Crystal data†					
Space group	$C2/m$	$C2/m$	$C2/m$	$C2/m$	$C2/m$
Crystal size (mm)	$0.1 \times 0.1 \times 0.1$	$0.1 \times 0.1 \times 0.1$	$0.1 \times 0.15 \times 0.05$	$0.1 \times 0.1 \times 0.05$	$0.05 \times 0.13 \times 0.1$
Cell parameters					
a (Å)	19.1129(6)	19.0935(4)	19.105(2)	19.1558(6)	19.174(3)
b (Å)	5.8963(5)	5.900(1)	5.9021(6)	5.9125(9)	5.9194(8)
c (Å)	8.818(1)	8.810(2)	8.8143(7)	8.844(1)	8.830(1)
β (°)	97.449(2)	97.540(7)	97.513(3)	97.448(4)	97.497(4)
V (Å^3)	985.3(2)	983.8(3)	985.4(2)	993.3(2)	993.6(2)
D_{calc} (g/cm^3)	3.197	3.261	3.217	3.244	3.219
Intensity measurements					
Radiation	MoKα	MoKα	MoKα	MoKα	MoKα
Monochromator	Graphite	Graphite	Graphite	Graphite	Graphite
Diffractometer	Rigaku R-AXIS RAPID IP	Rigaku R-AXIS RAPID IP	Rigaku R-AXIS RAPID IP	Rigaku R-AXIS RAPID IP	Rigaku R-AXIS RAPID IP
Scan type	ω scans	ω scans	ω scans	ω scans	ω scans
θ_{min} (°)	3.37	3.38	3.37	3.36	3.36
θ_{max} (°)	27.52	27.58	27.61	27.50	27.51
Data reduction					
No. of collected reflections	6147	6113	7204	7167	5488
No. of unique reflections	1243	1238	1248	1250	1243
Reflections $F_o > 4\sigma F_o$	1058	829	1070	1105	1095
R_{int}	0.051	0.074	0.124	0.0784	0.1050
Corrections	Lorentz-polarization absorption	Lorentz-polarization absorption	Lorentz-polarization absorption	Lorentz-polarization absorption	Lorentz-polarization absorption
μ (cm^{-1})	20.96	23.35	20.88	24.11	22.73
Structure solution and refinement					
Structure solution	Direct method	Direct method	Direct method	Direct method	Direct method
Miller index limits	$0 \leq h \leq 24, 0 \leq k \leq 7, -11 \leq l \leq 11$	$0 \leq h \leq 24, 0 \leq k \leq 7, -11 \leq l \leq 11$	$0 \leq h \leq 24, 0 \leq k \leq 7, -11 \leq l \leq 11$	$0 \leq h \leq 24, 0 \leq k \leq 7, -11 \leq l \leq 11$	$0 \leq h \leq 24, 0 \leq k \leq 7, -11 \leq l \leq 11$
Refinement system used	SHELXL-97 (Sheldrick 1997)	SHELXL-97 (Sheldrick 1997)	SHELXL-97 (Sheldrick 1997)	SHELXL-97 (Sheldrick 1997)	SHELXL-97 (Sheldrick 1997)
Refinement on	F^2	F^2	F^2	F^2	F^2
$R1$ (Unique reflections)	0.0484	0.081	0.0684	0.0736	0.0834
$R1$ ($F_o > 4\sigma F_o$)	0.0408	0.0502	0.0632	0.0692	0.0788
$wR2$	0.1337	0.1547	0.1747	0.2027	0.2024
S	1.088	0.954	1.039	1.564	1.583
No. of parameters	134	131	132	133	127
Weighting scheme	$w = 1/[\sigma^2(F_o^2) + (0.0922P)^2 + 0.00P]$ where $P = [Max(F_o^2,0) + 2F_c^2]/3$	$w = 1/[\sigma^2(F_o^2) + (0.0922P)^2 + 0.00P]$ where $P = [Max(F_o^2,0) + 2F_c^2]/3$	$w = 1/[\sigma^2(F_o^2) + (0.1214P)^2 + 0.00P]$ where $P = [Max(F_o^2,0) + 2F_c^2]/3$	$w = 1/[\sigma^2(F_o^2) + (0.0922P)^2 + 0.00P]$ where $P = [Max(F_o^2,0) + 2F_c^2]/3$	$w = 1/[\sigma^2(F_o^2) + (0.0922P)^2 + 0.00P]$ where $P = [Max(F_o^2,0) + 2F_c^2]/3$
$(\Delta/\sigma)_{max}$	0.0009	0.0059	0.0030	0.0073	0.0003
$\Delta\rho_{max}$ (e Å^{-3})	0.678	1.289	1.221	1.41	1.670
$\Delta\rho_{min}$ (e Å^{-3})	−0.894	−1.436	−1.223	−1.26	−1.46

* Unit-cell parameters were measured at 293 K. Diffraction data were collected at 293 K.
† ocp1211: $Na_{0.13}K_{0.02}Ba_{0.02}Ca_{7.70}Mg_{1.88}Mn_{0.05}Ni_{0.02}Fe_{0.38}V_{0.03}Cr_{0.52}Al_{9.04}Ti_{0.07}Si_{12.15}O_{56}H_{15.64}$ ($Z = 1$);
ocp0604: $Na_{0.16}K_{0.03}Ba_{0.01}Ca_{7.47}Mg_{1.81}Mn_{0.04}Ni_{0.01}Fe_{0.18}V_{0.01}Cr_{1.65}Al_{8.60}Ti_{0.01}Si_{12.01}O_{56}H_{15.04}$ ($Z = 1$);
ocp1028: $Na_{0.25}K_{0.03}Ca_{7.90}Mg_{1.60}Mn_{0.03}Ni_{0.01}Fe_{0.13}V_{0.01}Cr_{1.26}Al_{7.99}Ti_{0.01}Si_{12.76}O_{56}H_{14.36}$ ($Z = 1$);
ocp1013: $Na_{0.13}K_{0.02}Ca_{7.83}Mg_{1.79}Mn_{0.08}Ni_{0.01}Fe_{0.33}V_{0.03}Cr_{1.94}Al_{7.98}Si_{11.84}O_{56}H_{14.51}$ ($Z = 1$);
ocp1016: $Na_{0.15}K_{0.02}Ca_{7.64}Mg_{1.94}Mn_{0.08}Fe_{0.37}V_{0.03}Cr_{1.43}Al_{8.69}Ti_{0.01}Si_{11.65}O_{56}H_{14.71}$ ($Z = 1$) where H was calculated based on the charge balance.

observed site-scattering values (Hawthorne et al. 1995). The site-scattering values were derived from the site occupancy of Al at the X and Y sites refined without any constraint. The site populations at the X and Y sites were derived using the following assumptions: (1) elements with abundances less than 0.01
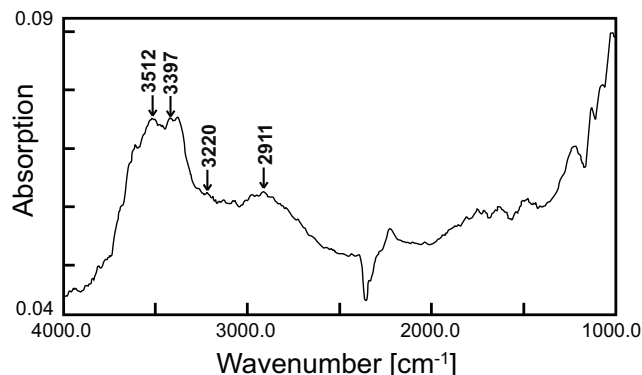

FIGURE 1. Infrared spectrum of chromian pumpellyite in the range between 4000 and 1500 cm^{-1}.

apfu were not considered; (2) Mg, Fe^{2+}, Mn^{2+}, and Ni^{2+} were assigned to X, based on the results of previous TOF neutron and X-ray Rietveld analyses (Nagashima and Akasaka 2007), Mössbauer studies (Akasaka et al. 1997; Artioli et al. 2003), and X-ray single-crystal study (Yoshiasa and Matsumoto 1985); (3) V^{3+} and Ti^{4+} to Y after Brigatti et al. (2006). The structural formulae constructed based on the results of the present study are: $Ca_8(Mg_{1.88}Al_{1.51}Fe^{2+}_{0.38}Cr_{0.16}Mn^{2+}_{0.05}Ni_{0.02})_{\Sigma4.00}(Al_{7.90}Ti_{0.07}V_{0.03})_{\Sigma8.00}$ $Si_{12}O_{40.36}(OH)_{15.64}$ for ocp1211, $Ca_8(Mg_{1.81}Al_{1.53}Cr_{0.42}Fe^{2+}_{0.18}Mn^{2+}_{0.04}$ $Ni_{0.01})_{\Sigma3.99}(Al_{7.34}Cr_{0.65}V_{0.01})_{\Sigma8.00}Si_{12}O_{40.96}(OH)_{15.04}$ for ocp0604, $Ca_8(Al_{1.62}Mg_{1.60}Cr_{0.61}Fe^{2+}_{0.13}Mn^{2+}_{0.03}Ni_{0.01})_{\Sigma4.00}(Al_{7.36}Cr_{0.61}V_{0.03})_{\Sigma8.00}$ $Si_{12}O_{41.61}(OH)_{14.36}$ for ocp1028, $Ca_8(Mg_{1.79}Al_{1.33}Cr_{0.47}Fe^{2+}_{0.33}$ $Mn^{2+}_{0.08})_{\Sigma4.00}(Al_{6.66}Cr_{1.31}V_{0.03})_{\Sigma8.00}Si_{12}O_{41.49}(OH)_{14.51}$ for ocp1013, $Ca_8(Mg_{1.94}Al_{1.23}Cr_{0.38}Fe^{2+}_{0.37}Mn^{2+}_{0.08})_{\Sigma4.00}(Al_{6.72}Cr_{1.25}V_{0.03})_{\Sigma8.00}$ $Si_{12}O_{40.29}(OH)_{14.72}$ for ocp1016. For all samples, the Cr contents derived from the site-scattering values deviate somewhat from those obtained from the EPMA analysis. To verify the determined site populations and structural models, bond-valence sums were calculated using the function of the electrostatic strength defined by Brown and Altermatt (1985) and the bond-valence parameters of Brese and O'Keeffe (1991). Table 7 shows the results of the

TABLE 3. Atomic positions and isotropic displacement parameters ($Å^2$)*

Atom		ocp1211	ocp0604	ocp1028	ocp1013	ocp1016	Atom		ocp1211	ocp0604	ocp1028	ocp1013	ocp1016
W1	x	0.33945(6)	0.33949(9)	0.33946(6)	0.33942(6)	0.33953(7)	O5	x	0.4577(2)	0.4579(3)	0.4581(2)	0.4570(2)	0.4573(2)
	y	1/2	1/2	1/2	1/2	1/2		y	0	0	0	0	0
	z	0.25010(13)	0.2504(2)	0.25015(14)	0.25044(17)	0.25077(16)		z	0.1325(5)	0.1322(7)	0.1319(5)	0.1318(6)	0.1321(5)
	U_{eq}	0.0143(3)	0.0124(5)	0.0140(4)	0.0250(5)	0.0195(6)		U_{eq}	0.0147(8)	0.0121(14)	0.0144(9)	0.0256(10)	0.0179(10)
W2	x	0.15449(6)	0.1547(10)	0.15447(7)	0.15450(6)	0.15443(8)	O6	x	0.04494(19)	0.0445(3)	0.0445(2)	0.0443(2)	0.0451(2)
	y	1/2	1/2	1/2	1/2	1/2		y	1/2	1/2	1/2	1/2	1/2
	z	0.19087(15)	0.1902(2)	0.19028(16)	0.19028(18)	0.19033(18)		z	0.3702(4)	0.3691(7)	0.3699(4)	0.3689(5)	0.3692(5)
	U_{eq}	0.0181(3)	0.0157(5)	0.0173(4)	0.0286(6)	0.0230(6)		U_{eq}	0.0127(8)	0.0091(13)	0.0119(9)	0.0239(10)	0.0193(10)
X	x	1/4	1/4	1/4	1/4	1/4	O7	x	0.0333(2)	0.0331(3)	0.0327(2)	0.0338(2)	0.0337(3)
	y	1/4	1/4	1/4	1/4	1/4		y	0	0	0	0	0
	z	1/2	1/2	1/2	1/2	1/2		z	0.3677(4)	0.3679(7)	0.3679(5)	0.3703(6)	0.3694(6)
	U_{eq}	0.0141(5)	0.0105(8)	0.0138(6)	0.0242(7)	0.0197(7)		U_{eq}	0.0149(8)	0.0125(14)	0.0159(9)	0.0258(10)	0.0219(11)
Y	x	0.49561(5)	0.49569(8)	0.49567(6)	0.49572(6)	0.49569(6)	O8	x	0.1754(2)	0.1758(3)	0.1755(2)	0.1758(2)	0.1759(2)
	y	0.24602(19)	0.2461(3)	0.24622(19)	0.24633(18)	0.24607(19)		y	0	0	0	0	0
	z	0.25485(11)	0.25461(18)	0.2549(1)	0.25492(14)	0.25472(13)		z	0.0356(4)	0.0365(7)	0.0366(5)	0.0364(5)	0.0362(5)
	U_{eq}	0.0088(4)	0.0093(6)	0.0103(5)	0.0198(5)	0.0157(5)		U_{eq}	0.0161(8)	0.0109(13)	0.0147(9)	0.0255(10)	0.0205(10)
Z1	x	0.08985(7)	0.08983(13)	0.08974(8)	0.08990(8)	0.09000(9)	O9	x	0.1761(2)	0.1762(3)	0.1760(2)	0.1761(2)	0.1752(3)
	y	0	0	0	0	0		y	1/2	1/2	1/2	1/2	1/2
	z	0.05072(17)	0.0501(3)	0.05028(18)	0.0502(2)	0.0505(2)		z	0.4779(4)	0.4788(7)	0.4779(5)	0.4793(6)	0.4773(6)
	U_{eq}	0.0113(4)	0.0099(5)	0.0101(4)	0.0222(5)	0.0167(5)		U_{eq}	0.0156(8)	0.0148(14)	0.0159(9)	0.0287(11)	0.0243(11)
Z2	x	0.24752(8)	0.24745(13)	0.24766(8)	0.24740(9)	0.24745(10)	O10	x	0.3131(2)	0.3130(3)	0.3132(2)	0.3138(2)	0.3134(3)
	y	0	0	0	0	0		y	0	0	0	0	0
	z	0.16555(17)	0.1661(3)	0.16570(18)	0.1655(2)	0.1659(2)		z	0.0664(5)	0.0674(7)	0.0654(5)	0.0680(6)	0.0674(6)
	U_{eq}	0.0119(4)	0.0101(6)	0.0110(4)	0.0230(5)	0.0180(5)		U_{eq}	0.0203(9)	0.0199(16)	0.0203(10)	0.0300(11)	0.0261(12)
Z3	x	0.40308(7)	0.40294(12)	0.40311(8)	0.40304(8)	0.40310(9)	O11	x	0.1852(2)	0.1856(3)	0.1854(2)	0.1854(2)	0.1851(2)
	y	0	0	0	0	0		y	0	0	0	0	0
	z	0.46562(16)	0.4660(3)	0.46569(17)	0.4660(2)	0.4657(2)		z	0.4971(4)	0.4988(7)	0.4975(5)	0.4988(6)	0.4990(5)
	U_{eq}	0.0109(4)	0.0091(5)	0.0106(4)	0.0219(5)	0.0167(5)		U_{eq}	0.0166(9)	0.01435(14)	0.0127(9)	0.0298(11)	0.0209(10)
O1	x	0.07094(14)	0.0706(2)	0.07104(15)	0.07125(15)	0.07116(17)	H5	x	–	0.4064(19)	–	–	–
	y	0.2253(5)	0.2242(7)	0.2242(6)	0.2247(6)	0.2253(6)		y	–	0	–	–	–
	z	0.1372(3)	0.1375(5)	0.1369(3)	0.1368(4)	0.1366(4)		z	–	0.13(4)	–	–	–
	U_{eq}	0.0155(6)	0.0132(10)	0.0138(7)	0.0250(8)	0.0210(8)		U_{eq}	–	0.05	–	–	–
O2	x	0.24570(13)	0.24608(19)	0.24594(15)	0.24590(15)	0.2459(17)	H7	x	0.035(4)	0.050(4)	0.44(5)	–	–
	y	0.2317(5)	0.2297(7)	0.2299(6)	0.2316(6)	0.2315(6)		y	0	0	0	–	–
	z	0.2659(3)	0.2662(5)	0.2658(3)	0.2657(4)	0.2654(4)		z	0.4792(9)	0.4780(19)	0.4797(10)	–	–
	U_{eq}	0.0146(6)	0.0138(10)	0.0158(7)	0.0268(8)	0.0232(9)		U_{eq}	0.05	0.05	0.05	–	–
O3	x	0.41746(14)	0.4175(2)	0.41682(16)	0.41705(15)	0.41680(17)	H10	x	0.362(3)	–	–	–	0.320(6)
	y	0.2236(5)	0.2215(7)	0.2223(6)	0.2230(5)	0.2227(6)		y	0	–	–	–	0
	z	0.3669(3)	0.3676(5)	0.3672(3)	0.3672(4)	0.3666(4)		z	0.118(17)	–	–	–	0.1794(6)
	U_{eq}	0.0152(6)	0.0131(10)	0.0148(7)	0.0243(7)	0.0197(8)		U_{eq}	0.05	–	–	–	0.05
O4	x	0.44478(19)	0.4449(3)	0.4450(2)	0.4452(2)	0.4452(2)	H11	x	0.1338(9)	–	0.1375(17)	–	–
	y	1/2	1/2	1/2	1/2	1/2		y	0	–	0	–	–
	z	0.1306(4)	0.1309(7)	0.1305(4)	0.1319(5)	0.1313(5)		z	0.471(19)	–	0.442(8)	–	–
	U_{eq}	0.0114(8)	0.0093(13)	0.0132(9)	0.0211(9)	0.0173(10)		U_{eq}	0.05	–	0.05	–	–

* Isotropic displacement parameters (U_{eq}) of hydrogen was fixed at 0.05 $Å^2$.

TABLE 4. Anisotropic displacement parameters (Å^2)

Atom	U_{ij}	ocp1211	ocp0604	ocp1028	ocp1013	ocp1016	Atom	U_{ij}	ocp1211	ocp0604	ocp1028	ocp1013	ocp1016
W1	U_{11}	0.0120(5)	0.0099(9)	0.0095(6)	0.0100(8)	0.0185(8)	O3	U_{11}	0.0164(13)	0.013(2)	0.0117(14)	0.0143(14)	0.0205(15)
	U_{22}	0.0174(6)	0.0154(10)	0.0184(7)	0.0291(8)	0.0200(9)		U_{22}	0.0146(14)	0.012(2)	0.0188(17)	0.0268(16)	0.0194(17)
	U_{33}	0.0140(5)	0.0121(9)	0.0144(6)	0.0381(8)	0.0212(8)		U_{33}	0.0154(13)	0.014(2)	0.0139(13)	0.0345(16)	0.0199(15)
	U_{23}	0	0	0	0	0		U_{23}	0.0021(11)	−0.0004(19)	0.0025(12)	0.0033(14)	0.0012(13)
	U_{13}	0.0030(4)	0.0023(7)	0.0026(4)	0.0111(5)	0.0065(5)		U_{13}	0.0050(10)	0.0009(17)	0.0024(10)	0.0134(12)	0.0056(12)
	U_{12}	0	0	0	0	0		U_{12}	0.0002(11)	0.0020(19)	0.0003(11)	0.0017(12)	0.0015(13)
W2	U_{11}	0.0130(6)	0.0104(9)	0.0116(7)	0.0120(8)	0.0204(9)	O4	U_{11}	0.0078(16)	0.004(3)	0.0096(19)	0.0089(19)	0.017(2)
	U_{22}	0.0142(6)	0.0100(10)	0.0134(7)	0.0260(8)	0.0169(8)		U_{22}	0.0129(18)	0.014(3)	0.020(2)	0.025(2)	0.015(2)
	U_{33}	0.0265(7)	0.0257(11)	0.0265(7)	0.0489(10)	0.0314(9)		U_{33}	0.0127(17)	0.009(3)	0.0086(17)	0.030(2)	0.021(2)
	U_{23}	0	0	0	0	0		U_{23}	0	0	0	0	0
	U_{13}	0.0006(4)	−0.0013(8)	0.0004(5)	0.0084(6)	0.0025(6)		U_{13}	−0.0010(13)	−0.004(2)	−0.0023(14)	0.0060(16)	0.0051(17)
	U_{12}	0	0	0	0	0		U_{12}	0	0	0	0	0
X	U_{11}	0.0149(8)	0.0137(13)	0.0122(9)	0.0125(10)	0.0204(10)	O5	U_{11}	0.0131(19)	0.005(3)	0.014(2)	0.013(2)	0.019(2)
	U_{22}	0.0133(8)	0.0065(12)	0.0146(10)	0.0245(11)	0.0167(11)		U_{22}	0.015(2)	0.018(3)	0.019(2)	0.026(2)	0.018(2)
	U_{33}	0.0145(8)	0.0116(12)	0.0150(9)	0.0378(11)	0.0228(11)		U_{33}	0.0155(18)	0.012(3)	0.0098(18)	0.039(3)	0.018(2)
	U_{23}	0.0005(6)	0.0004(10)	0.0003(6)	−0.0009(7)	0.0007(6)		U_{23}	0	0	0	0	0
	U_{13}	0.0029(5)	0.0025(9)	0.0034(6)	0.0119(7)	0.0067(7)		U_{13}	0.0000(15)	−0.002(2)	−0.0012(16)	0.0066(19)	0.0060(18)
	U_{12}	−0.0002(6)	−0.0001(10)	−0.0003(6)	−0.0011(6)	−0.0003(7)		U_{12}	0	0	0	0	0
Y	U_{11}	0.0092(6)	0.0080(9)	0.0094(7)	0.0077(7)	0.0163(8)	O6	U_{11}	0.0119(18)	0.001(3)	0.0074(19)	0.013(2)	0.019(2)
	U_{22}	0.0090(7)	0.0109(10)	0.0113(8)	0.0203(8)	0.0133(8)		U_{22}	0.0124(19)	0.015(3)	0.018(2)	0.024(2)	0.017(2)
	U_{33}	0.0088(6)	0.0091(9)	0.0104(7)	0.0332(8)	0.0181(8)		U_{33}	0.0144(18)	0.010(3)	0.0101(17)	0.037(2)	0.023(2)
	U_{23}	−0.0000(4)	0.0010(8)	0.0004(4)	0.0010(5)	−0.0000(4)		U_{23}	0	0	0	0	0
	U_{13}	0.0032(4)	0.0018(6)	0.0016(4)	0.0098(5)	0.0050(5)		U_{13}	0.0037(14)	−0.003(2)	−0.0003(14)	0.0092(18)	0.0060(18)
	U_{12}	0.0007(4)	0.0000(7)	−0.0002(4)	0.0007(4)	0.0003(4)		U_{12}	0	0	0	0	0
Z1	U_{11}	0.0104(7)	0.0078(12)	0.0098(8)	0.0072(8)	0.0163(9)	O7	U_{11}	0.0170(19)	0.008(3)	0.014(2)	0.014(2)	0.028(3)
	U_{22}	0.0125(7)	0.0133(12)	0.0107(9)	0.0252(10)	0.0164(10)		U_{22}	0.015(2)	0.019(4)	0.020(2)	0.028(2)	0.018(2)
	U_{33}	0.0113(7)	0.0080(12)	0.0096(7)	0.0358(10)	0.0177(9)		U_{33}	0.0129(18)	0.010(3)	0.0131(19)	0.035(2)	0.021(2)
	U_{23}	0	0	0	0	0		U_{23}	0	0	0	0	0
	U_{13}	0.0020(5)	−0.0006(9)	0.0008(6)	0.0087(7)	0.0039(7)		U_{13}	0.0027(15)	−0.002(2)	0.0009(16)	0.0031(18)	0.0041(19)
	U_{12}	0	0	0	0	0		U_{12}	0	0	0	0	0
Z2	U_{11}	0.0120(7)	0.0074(12)	0.0098(8)	0.0105(8)	0.0196(9)	O8	U_{11}	0.0126(18)	0.012(3)	0.014(2)	0.0080(19)	0.020(2)
	U_{22}	0.0119(7)	0.0114(13)	0.0110(8)	0.0246(9)	0.0163(9)		U_{22}	0.022(2)	0.009(3)	0.018(2)	0.036(2)	0.026(2)
	U_{33}	0.0118(7)	0.0108(12)	0.0120(8)	0.0351(10)	0.0183(9)		U_{33}	0.0132(18)	0.011(3)	0.0118(18)	0.033(2)	0.017(2)
	U_{23}	0	0	0	0	0		U_{23}	0	0	0	0	0
	U_{13}	0.0010(5)	−0.0015(9)	0.0009(6)	0.0082(7)	0.0036(7)		U_{13}	−0.0001(14)	0.001(2)	−0.0001(15)	0.0057(2)	0.0059(17)
	U_{12}	0	0	0	0	0		U_{12}	0	0	0	0	0
Z3	U_{11}	0.0096(7)	0.0079(12)	0.0106(8)	0.0081(8)	0.0164(9)	O9	U_{11}	0.0128(18)	0.012(3)	0.012(2)	0.008(2)	0.018(2)
	U_{22}	0.0128(8)	0.0124(12)	0.0105(9)	0.0249(10)	0.0166(10)		U_{22}	0.022(2)	0.026(4)	0.022(2)	0.038(3)	0.031(3)
	U_{33}	0.0103(7)	0.0071(12)	0.0106(8)	0.0346(10)	0.0181(9)		U_{33}	0.0122(18)	0.008(3)	0.0140(19)	0.042(3)	0.024(2)
	U_{23}	0	0	0	0	0		U_{23}	0	0	0	0	0
	U_{13}	0.0012(5)	0.0009(9)	0.0013(6)	0.0096(7)	0.0068(7)		U_{13}	0.0023(14)	0.003(2)	0.0016(16)	0.0096(18)	0.0060(19)
	U_{12}	0	0	0	0	0		U_{12}	0	0	0	0	0
O1	U_{11}	0.0152(13)	0.015(2)	0.0087(14)	0.0127(14)	0.0184(16)	O10	U_{11}	0.0127(19)	0.010(3)	0.012(2)	0.012(2)	0.023(2)
	U_{22}	0.0148(14)	0.014(2)	0.0189(16)	0.0266(16)	0.0201(17)		U_{22}	0.030(3)	0.034(4)	0.031(3)	0.043(3)	0.038(3)
	U_{33}	0.0176(13)	0.011(2)	0.0146(13)	0.0380(17)	0.0253(16)		U_{33}	0.018(2)	0.015(3)	0.018(2)	0.037(2)	0.018(2)
	U_{23}	−0.0028(11)	0.0021(19)	−0.0030(12)	−0.0014(13)	0.0009(13)		U_{23}	0	0	0	0	0
	U_{13}	0.0066(10)	0.0022(16)	0.0039(10)	0.0122(12)	0.0063(13)		U_{13}	0.0040(16)	0.001(3)	0.0017(16)	0.0091(18)	0.0069(19)
	U_{12}	−0.0004(11)	−0.0024(19)	−0.0004(11)	−0.0019(12)	0.0008(13)		U_{12}	0	0	0	0	0
O2	U_{11}	0.0151(13)	0.012(2)	0.0112(15)	0.0133(15)	0.0240(18)	O11	U_{11}	0.0150(19)	0.016(3)	0.0074(19)	0.011(2)	0.019(2)
	U_{22}	0.0113(13)	0.013(2)	0.0167(17)	0.0278(18)	0.0174(18)		U_{22}	0.020(2)	0.014(3)	0.018(2)	0.037(3)	0.026(2)
	U_{33}	0.0167(13)	0.015(2)	0.0188(14)	0.0410(18)	0.0286(19)		U_{33}	0.0152(19)	0.011(3)	0.0140(19)	0.044(3)	0.020(2)
	U_{23}	−0.0018(11)	0.0036(19)	−0.0014(12)	−0.0023(13)	−0.0015(14)		U_{23}	0	0	0	0	0
	U_{13}	−0.0008(10)	−0.0019(17)	−0.0014(12)	0.0096(13)	0.0050(14)		U_{13}	0.0019(15)	0.004(3)	0.0055(14)	0.0123(19)	0.0098(18)
	U_{12}	0.0008(11)	−0.001(2)	0.0008(11)	−0.0007(11)	0.0031(13)		U_{12}	0	0	0	0	0

bond-valence summations for the refined site populations at the X and Y sites with the interatomic distances derived from the refined atomic positions. Thus, the discrepancies in Cr contents may be attributed to the inhomogeneous composition of the Osayama chromian pumpellyites. The bond-valence sums of O5, O7, O10, and O11 are close to 1, indicating that the hydroxyl groups in the Osayama chromian pumpellyites are located in these positions. However, the valence sums of O10 and O11 are 1.3–1.4, somewhat >1. Thus, the hydroxyl group and oxygen can both be assigned to these sites (Fig. 2).

DISCUSSION
Behavior of chromium in pumpellyite

Because of the rare occurrence of chromian pumpellyite and the difficulty of its synthesis, the distribution of Cr among the oc-tahedral X and Y sites was not known until the X-ray and neutron diffraction structural refinements of Sarani chromian pumpellyite (3.76 apfu Cr) by Nagashima and Akasaka (2007). They found that Cr^{3+} ions were distributed in both the X and Y sites with a $Cr_X:Cr_Y$ ratio of 1.28:2.48 (apfu), and that the distribution coefficient of Cr^{3+} against Al between the X and Y sites [defined as $K_D = (Cr_X/Al_X)/(Cr_Y/Al_Y)$] was 3.56. These results supported the X-ray single-crystal study of Sarani chromian pumpellyite crystal with total Cr of 3.30 apfu by Nagashima (2006), which yielded values of $Cr_X:Cr_Y = 1.232:2.064$ and $K_D = 4.39$.

In Osayama chromian pumpellyites ocp0604 (1.07 total Cr apfu), ocp1028 (1.22 total Cr apfu), ocp1013 (1.78 total Cr apfu), and ocp1016 (1.63 total Cr apfu) (Table 8), Cr^{3+} cations are also distributed in both the X and Y sites: the $Cr_X:Cr_Y$ ratios are 0.42:0.65, 0.61:0.61, 0.47:1.31, and 0.38:1.25 (apfu), respec-

tively (Table 6). In ocp1211 (0.16 total Cr apfu), Cr^{3+} ions are distributed exclusively in the X site. The Cr populations in the X and Y sites are well correlated with total Cr contents in the chromian pumpellyites, as illustrated in Figure 3a:

Cr_X (apfu) = 0.3258[Total Cr (apfu)] + 0.048 (R^2 = 0.90),
Cr_Y (apfu) = 0.674[Total Cr (apfu)] – 0.051 (R^2 = 0.98).

Although the increasing rate of Cr population in the Y site (0.674 apfu/total Cr apfu) is greater than that in the X site (0.3258 apfu/total Cr apfu), this does not imply a stronger preference of Cr for the Y site than the X site, because the number of equivalent Y sites is twice of that of the X site, and almost a half of the X site is filled with divalent cations.

The site preference of Cr is well represented by the ratio of Cr against Al in the X and Y site, that is $(Cr/Al)_X$ and $(Cr/Al)_Y$,

respectively. As shown in Figure 3b, $(Cr/Al)_X$ and $(Cr/Al)_Y$, are correlated with total Cr (apfu) by the relationships:

$(Cr/Al)_X$ = 0.1167[Total Cr (apfu)]^2
    – 0.0142[Total Cr (apfu)] + 0.1165 (R^2 = 0.97),
$(Cr/Al)_Y$ = 0.1233[Total Cr (apfu)] – 0.0344 (R^2 = 0.98).

The preference of Cr for the X site is thus greater than that for the Y site, and increases rapidly with increasing total Cr content. The K_D values of ocp0604, ocp1028, ocp1013, ocp1016, and Sarani chromian pumpellyite (Nagashima 2006) with 3.09, 4.54, 1.79, 1.66, and 4.39, respectively (Table 8), also indicate stronger preference of Cr for the X site than the Y site. Although the variation of K_D values with increasing total Cr content (apfu) is not necessarily systematic, a rapid increase of $(Cr/Al)_X$ with Cr content in contrast to a linear increase of $(Cr/Al)_Y$ suggests the K_D values tend to increase with increasing Cr content. These results reaffirm that the assumption of Ivanov et al. (1981) that Cr^{3+} ions prefer the Y site is incorrect.

Variation of interatomic distances and unit-cell parameters caused by the ionic substitution of Cr^{3+} for Al^{3+}

The structural changes caused by ionic substitution at the Y site can be represented in terms of the Y-O distance and mean ionic radius at that site (Nagashima and Akasaka 2007). As shown in Figure 4, although the Y-O4 and -O6 distances do not depend on the mean ionic radius, the Y-O1, Y-O3, Y-O5, and Y-O7 distances increase with the increase of the mean ionic radius in the Y site, which results in the increase of the mean Y-O distance (Fig. 5). It is noted that the mean Y-O distances of Osayama chromian pumpellyites lie on a regression line of mean Y-O distances against mean ionic radius for various pumpellyites.

Insensitive property of the XO_6-octahedra with the ionic substitution in the X site and non-systematic variation of mean X-O distances with mean ionic radius have been shown by Nagashima et al. (2006) and Nagashima and Akasaka (2007), which was interpreted in terms of the essentially large size of the XO_6-octahedra and their geometric relationship with W1 and W2 polyhedra. The X-O_i distances of Osayama chromian pumpellyites also do not show distinct variation even though the range of the mean ionic radius at the X site attains almost twice of that at the Y site (Figs. 4 and 5), although the X-O9 and -O11 distances show very weak increasing tend with the increase of the mean ionic radius. Consequently, increase in the Y-O distance

TABLE 5. Selected interatomic distances (Å)

			ocp1211	ocp0604	ocp1028	ocp1013	ocp1016
Y	O1		1.888(3)	1.879(4)	1.891(3)	1.899(3)	1.898(4)
	O3		1.899(3)	1.906(4)	1.913(3)	1.914(3)	1.916(4)
	O4		2.027(3)	2.024(4)	2.026(3)	2.024(3)	2.027(3)
	O5		1.895(3)	1.894(4)	1.897(3)	1.910(3)	1.905(3)
	O6		1.944(3)	1.936(4)	1.940(3)	1.939(3)	1.947(3)
	O7		1.888(3)	1.887(4)	1.885(3)	1.905(3)	1.903(3)
Average			1.924(3)	1.921(4)	1.925(3)	1.936(3)	1.933(3)
X	O2	×2	2.058(3)	2.055(4)	2.059(3)	2.067(3)	2.066(4)
	O9	×2	2.033(3)	2.032(4)	2.035(3)	2.038(3)	2.053(3)
	O11	×2	1.924(3)	1.920(4)	1.922(3)	1.927(3)	1.933(3)
Average			2.005(3)	2.002(4)	2.005(3)	2.011(3)	2.017(3)
W1	O2	×2	2.408(3)	2.410(4)	2.412(3)	2.410(3)	2.413(4)
	O3	×2	2.354(3)	2.362(4)	2.353(3)	2.358(3)	2.354(4)
	O4		2.390(4)	2.390(6)	2.395(4)	2.400(4)	2.403(5)
	O8		2.498(4)	2.506(6)	2.506(4)	2.516(5)	2.513(5)
	O11		2.337(4)	2.322(6)	2.334(4)	2.328(5)	2.319(5)
Average			2.393(3)	2.395(5)	2.395(3)	2.397(4)	2.396(4)
W2	O1	×2	2.281(3)	2.287(4)	2.284(3)	2.285(3)	2.285(4)
	O2	×2	2.384(3)	2.396(4)	2.395(3)	2.393(3)	2.397(4)
	O6		2.782(4)	2.786(6)	2.791(4)	2.796(5)	2.784(5)
	O9		2.511(4)	2.522(7)	2.515(4)	2.536(5)	2.513(5)
	O10		2.427(4)	2.430(7)	2.413(5)	2.439(5)	2.435(5)
Average			2.436(4)	2.443(5)	2.439(4)	2.447(4)	2.442(4)
Z1	O1	×2	1.596(3)	1.597(5)	1.592(3)	1.597(3)	1.599(4)
	O4		1.649(4)	1.644(6)	1.644(4)	1.663(5)	1.658(5)
	O8		1.658(4)	1.661(6)	1.659(5)	1.666(4)	1.668(5)
Average			1.625(4)	1.625(6)	1.622(4)	1.631(5)	1.633(5)
Z2	O2	×2	1.630(3)	1.619(5)	1.621(3)	1.633(4)	1.630(4)
	O8		1.674(4)	1.663(6)	1.669(4)	1.667(5)	1.669(5)
	O10		1.619(4)	1.615(7)	1.624(5)	1.627(5)	1.625(5)
Average			1.638(4)	1.629(6)	1.633(4)	1.640(5)	1.638(5)
Z3	O3	×2	1.623(3)	1.612(5)	1.613(3)	1.623(3)	1.623(4)
	O6		1.646(4)	1.653(6)	1.650(4)	1.665(5)	1.653(5)
	O9		1.654(4)	1.647(7)	1.652(5)	1.651(4)	1.644(5)
Average			1.636(4)	1.631(6)	1.632(4)	1.641(4)	1.636(5)

TABLE 6. Refined site-scattering values* and assigned site populations† for the X and Y sites

Sample	Site	MAN‡	N§	Site-scattering value (epfu)	Site populations (apfu)
ocp1211	X	14.44	4	57.76	1.88 Mg + 1.51 Al + 0.38 Fe^{2+} + 0.16 Cr + 0.05 Mn^{2+} + 0.02 Ni
	Y	13.05	8	104.38	7.90 Al + 0.07 Ti + 0.03 V
ocp0604	X	14.47	4	57.88	1.81 Mg + 1.53 Al + 0.42 Cr + 0.18 Fe^{2+} + 0.04 Mn^{2+} + 0.01 Ni
	Y	13.91	8	111.28	7.34 Al + 0.65 Cr + 0.01 V
ocp1028	X	14.82	4	59.28	1.62 Al + 1.60 Mg + 0.61 Cr + 0.13 Fe^{2+} + 0.03 Mn^{2+} + 0.01 Ni
	Y	13.87	8	110.96	7.36 Al + 0.61 Cr + 0.03 V
ocp1013	X	15.15	4	60.60	1.79 Mg + 1.33 Al + 0.47 Cr + 0.33 Fe^{2+} + 0.08 Mn^{2+}
	Y	14.84	8	118.72	6.66 Al + 1.31 Cr + 0.03 V
ocp1016	X	14.99	4	59.96	1.94 Mg + 1.23 Al + 0.38 Cr + 0.37 Fe^{2+} + 0.08 Mn^{2+}
	Y	14.75	8	118.00	6.72 Al + 1.25 Cr + 0.03 V

* The site-scattering values were defined from the site occupancies of Al at the X and Y sites refined without constraint.
† Cations less than 0.01 apfu were neglected. Fe^{2+} was assigned to the X site by the semi-quantitative analysis of Fe^{2+}/Fe^{3+} ratio.
‡ Mean atomic number.
§ Number of equivalent sites in the structural formula.

TABLE 7. Estimated bond-valence (vu) in chromian pumpellyite

	W1	W2	X	Y	Z1	Z2	Z3	$\Sigma_C v$	Anion
ocp1211 O1		0.428*		0.529	1.126*			2.083	O^{2-}
O2	0.304*	0.324*	0.351*			1.027*		2.006	O^{2-}
O3	0.351*			0.514			1.047*	1.912	O^{2-}
O4	0.319			0.364†	0.976			2.023	O^{2-}
O5				0.519†				1.038	OH^-
O6		0.111		0.455†			0.984	2.005	O^{2-}
O7				0.529†				1.058	OH^-
O8	0.238				0.953	0.912		2.103	O^{2-}
O9		0.230	0.376*†				0.963	1.945	O^{2-}
O10		0.288				1.058		1.347	O^{2-}, OH^-
O11	0.368		0.505*†					1.378	O^{2-}, OH^-
$\Sigma_A v$	2.235	2.133	2.464	2.910	4.181	4.024	4.041		
ocp0604 O1		0.421*		0.549	1.123*			2.093	O^{2-}
O2	0.302*	0.314*	0.349*			1.059*		2.024	O^{2-}
O3	0.344*			0.511			1.078*	1.933	O^{2-}
O4	0.319			0.371†	0.988			2.049	O^{2-}
O5				0.528†				1.056	OH^-
O6		0.109		0.470†			0.982	2.031	O^{2-}
O7				0.537†				1.074	OH^-
O8	0.233				0.945	0.939		2.117	O^{2-}
O9		0.223	0.371*†				0.964	1.929	O^{2-}
O10		0.286				1.071		1.357	O^{2-}, OH^-
O11	0.384		0.502*†					1.388	O^{2-}, OH^-
$\Sigma_A v$	2.228	2.088	2.444	2.966	4.179	4.128	4.102		
ocp1028 O1		0.425*		0.541	1.139*			2.105	O^{2-}
O2	0.300*	0.315*	0.343*			1.053*		2.011	O^{2-}
O3	0.352*			0.500			1.075*	1.927	O^{2-}
O4	0.315			0.369†	0.989			2.042	O^{2-}
O5				0.523†				1.046	OH^-
O6		0.108		0.465†			0.968	2.006	O^{2-}
O7				0.531†				1.062	OH^-
O8	0.233				0.950	0.925		2.108	O^{2-}
O9		0.228	0.366*†				0.975	1.935	O^{2-}
O10		0.299				1.043		1.342	O^{2-}, OH^-
O11	0.371		0.497*†					1.365	O^{2-}, OH^-
$\Sigma_A v$	2.223	2.115	2.412	2.929	4.217	4.074	4.093		
ocp1013 O1		0.424*		0.528	1.122*			2.074	O^{2-}
O2	0.302*	0.316*	0.347*			1.019*		1.984	O^{2-}
O3	0.348*			0.507			1.047*	1.902	O^{2-}
O4	0.310			0.377†	0.940			2.004	O^{2-}
O5				0.513†				1.026	OH^-
O6		0.106		0.474†			0.935	1.990	O^{2-}
O7				0.520†				1.040	OH^-
O8	0.227				0.930	0.930		2.087	O^{2-}
O9		0.215	0.376*†				0.971	1.937	O^{2-}
O10		0.279				1.036		1.315	O^{2-}, OH^-
O11	0.377		0.507*†					1.391	O^{2-}, OH^-
$\Sigma_A v$	2.214	2.080	2.460	2.919	4.114	4.004	4.000		
ocp1016 O1		0.423*		0.528	1.116*			2.067	O^{2-}
O2	0.300*	0.313*	0.350*			1.029*		1.992	O^{2-}
O3	0.352*			0.504			1.048*	1.904	O^{2-}
O4	0.308			0.373†	0.953			2.007	O^{2-}
O5				0.519†				1.038	OH^-
O6		0.110		0.463†			0.967	2.002	O^{2-}
O7				0.521†				1.042	OH^-
O8	0.229				0.928	0.925		2.082	O^{2-}
O9		0.229	0.363*†				0.989	1.944	O^{2-}
O10		0.282				1.042		1.324	O^{2-}, OH^-
O11	0.386		0.502*†					1.390	O^{2-}, OH^-
$\Sigma_A v$	2.227	2.093	2.430	2.908	4.113	4.025	4.052		

Notes: $\Sigma_A v$ is the valence of bonds emanating from cation summed over the bonded anions. $\Sigma_C v$ is the balance of bonds reaching anions.
* Two bonds per cation.
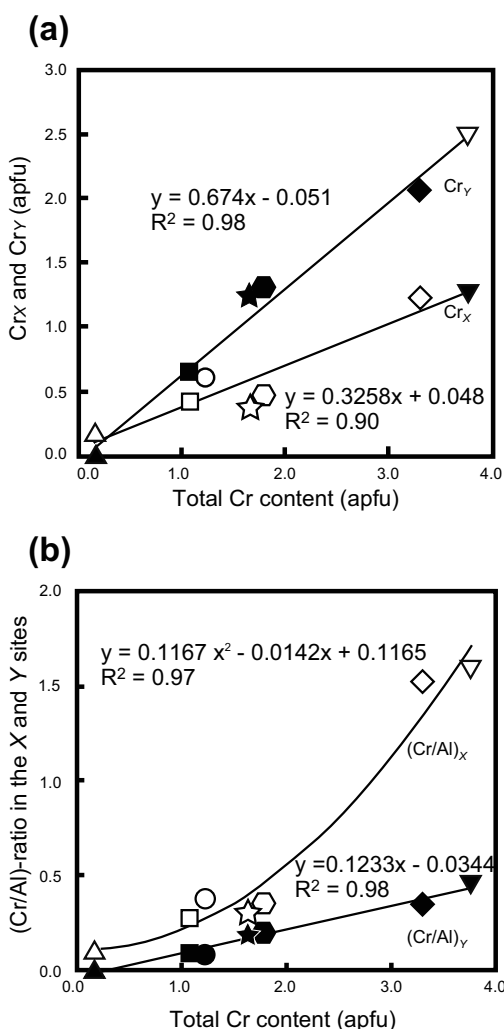† Two bonds per anion.

effects on the structural changes and cation substitutions at the X site do not cause systematic structural change.

Changes in the unit-cell parameters of pumpellyite with increasing Cr^{3+} content can be examined based on the unit-cell parameters of Osayama chromian pumpellyites with 0.16, 1.07, 1.22, 1.63, and 1.78 Cr^{3+} apfu (Table 8), and of Sarani chro-mian pumpellyites with 3.30 Cr^{3+} apfu [a = 19.18, b = 5.943, c = 8.807 Å, β = 97.44°; Nagashima (2006)] and 3.76 apfu (a = 19.1466–19.16, b = 5.932–5.9396, c = 8.813–8.819 Å, β = 97.603°; Nagashima and Akasaka 2007), where the unit-cell parameters of Sarani chromian pumpellyite in space group $A2/m$ by Nagashima (2006) and Nagashima and Akasaka (2007) were
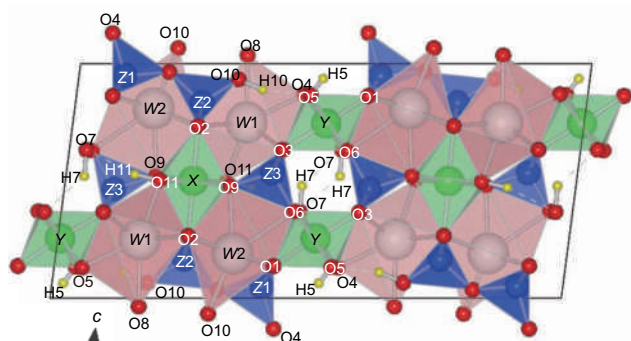
FIGURE 2. Crystal structure of chromian pumpellyite projected down [010] using the program VESTA (Momma and Izumi 2008). The H5 position is after Yoshiasa and Matsumoto (1985) and Nagashima and Akasaka (2007).
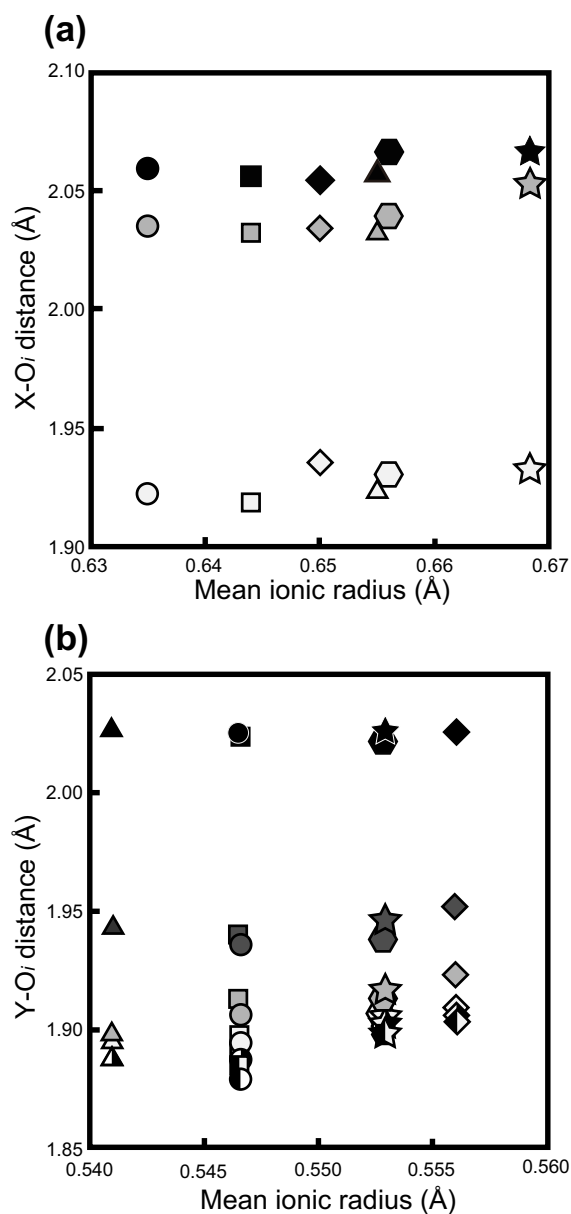
TABLE 8. Distribution coefficient K_D $[=(M^{3+}/Al^{3+})^X/(M^{3+}/Al^{3+})^Y]$ of pumpellyite

Pumpellyite	Refined Cr³⁺ (apfu)	K_D	References
Osayama ocp1211	0.16*	–	This study
Osayama ocp0604	1.07*	3.09	This study
Osayama ocp1028	1.22*	4.54	This study
Osayama ocp1013	1.78*	1.79	This study
Osayama ocp1016	1.63*	1.66	This study
Sarani chromian pumpellyite	3.30	4.39	Nagashima (2006)
Sarani chromian pumpellyite	3.76	3.56	Nagashima and Akasaka (2007)

* Total Cr content is refined by ShelXL97 (Sheldrick 1997).

FIGURE 3. (**a**) Relationships between total Cr content (atoms per formula unit: apfu) and Cr contents in the X and Y sites. (**b**) Relationships between total Cr content (apfu) and Cr/Al ratio in the X and Y sites. Open symbols are values for the X site, and closed symbols for Y site. Symbols and sources: triangles (ocp1211), squares (ocp0604), circles (ocp1028), hexagons (ocp1013), stars (ocp1016), diamonds (Nagashima 2006), and inverted triangle (Nagashima and Akasaka 2007). Regression lines were calculated from the single-crystal X-ray diffraction data.

FIGURE 4. The X-O$_i$ (**a**) and Y-O$_i$ (**b**) distances as a function of mean ionic radius. Mean ionic radii were calculated using the ionic radius values of Shannon (1976). (**a**) Closed symbols = O2; dark gray symbols = O9; and open symbols = O11. (**b**) Right filled symbols = O1; light gray symbols = O3; closed symbols = O4; left filled symbols = O5; dark gray symbols = O6; and open symbols = O7. Symbols and sources: triangles (ocp1211), squares (ocp0604), circles (ocp1028), hexagons (ocp1013), stars (ocp1016), and diamonds (Nagashima 2006).

(a)

$$y = 0.927x + 1.428$$
$$R^2 = 0.92$$

(b)
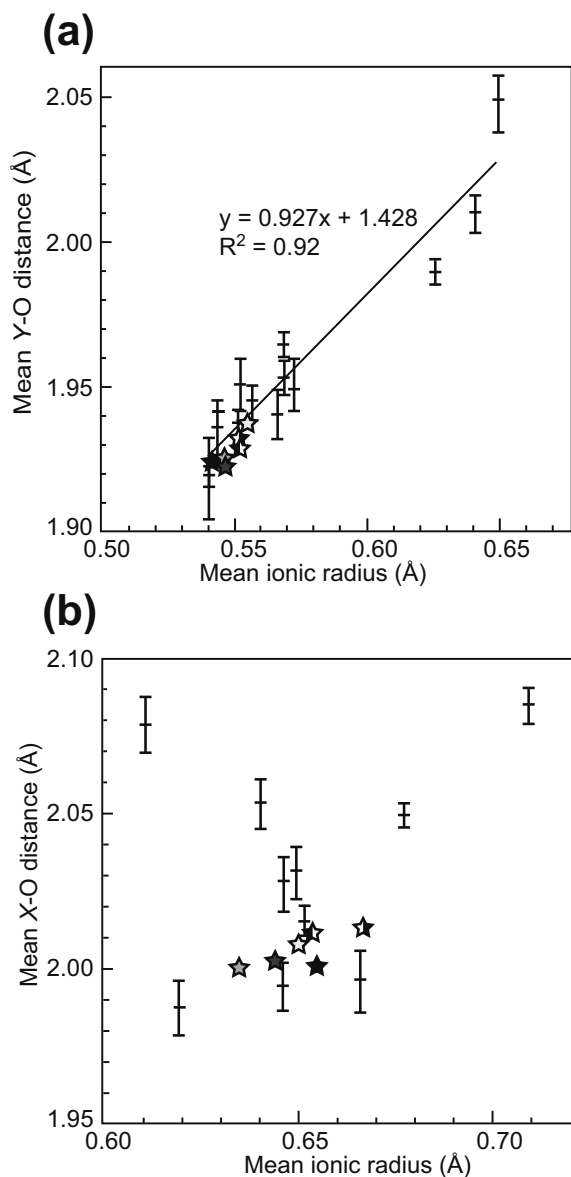
FIGURE 5. (**a**) The relationship between mean ionic radius at the Y site and mean Y-O distance. (**b**) The relationship between mean ionic radius at the X site and mean X-O distance. Mean ionic radii were calculated using the ionic radii of Shannon (1976). The space group of Nagashima (2006) is $A2/m$, thus we exchange a axis for c axis. Closed star (ocp1211), dark gray star (ocp0604), light gray star (ocp1028), left filled star (ocp1013), right filled star (ocp1016), and open star (Nagashima 2006). The data shown only by error bars are of other pumpellyite minerals (Galli and Alberti 1969; Allmann and Donnay 1973; Yoshiasa and Matsumoto 1985; Artioli and Geiger 1994; Artioli et al. 1996, 2003; Nagashima et al. 2006; Nagashima and Akasaka 2007). Details are shown in Nagashima and Akasaka (2007).

transformed to those of $C2/m$ in this paper. The relationships between the unit-cell parameters a, b, and c and Cr content are illustrated in Figure 6. The effective changes of the cell dimensions in chromian pumpellyite with increased number of Cr cations are evaluated with the absolute cell variation against total Cr content, which is the difference of the unit-cell parameters between chromian pumpellyites in this study and those of Mg-Al-pumpellyite
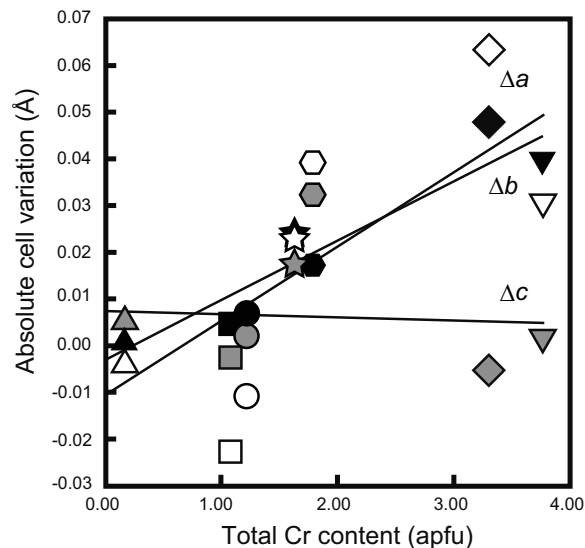
FIGURE 6. Absolute variations of unit-cell parameters in chromian pumpellyite as a function of total Cr content (apfu). Gray symbols refer to the a-axis, closed symbols b-axis, and open symbols c-axis. Symbols as in Figure 3.

(Yoshiasa and Matsumoto 1985). It is evident that the Δc of chromian pumpellyite does not depend on Cr content, whereas Δa and Δb increase with increasing Cr content, with slightly larger Δa-gradient than Δb. Contrary to the cell variation of chromian pumpellyite with the Cr content, the a, b, and c axes of Fe-rich pumpellyite all increase with increasing Fe content, with rates of increase becoming larger in the order c, b, a as shown in Figure 3 of Nagashima et al. (2006). [Note: the a and c axes with space group $A2/m$ in Nagashima et al. (2006) were transformed to the c and a axes of $C2/m$, respectively, in the present paper.] The cause of variation of the cell parameters with the substitution of Cr^{3+} for Al^{3+} can be attributed to the structural properties of the XO_6- and YO_6-octahedra, as discussed by Nagashima et al. (2006). These properties are: (1) the O1-O6, O3-O4, and O3-O5 edges of the YO_6-octahedra shared with WO_7-polyhedra prohibit the variation of the c axis; (2) the O1-O4, O1-O5, O3-O6, and O3-O7 not shared with other polyhedral cause the straightforward variation of the a axis; (3) variation of the b axis reflects the change of the YO_6-octahedra forming a chain along the b axis; and (4) due to the large size of the XO_6-octahedra and the edges of XO_6-octahedra shared with the W1- and W2-polyhedra, the XO_6-octahedra do not affect the systematic structural variation, even if some ionic substitution occurs in the X site. Because of the stronger preference of Cr^{3+} ion for the X site rather than the Y site and the smaller ionic radius of Cr^{3+} than that of Fe^{3+}, the variation of the a axis caused by the substitution of Cr^{3+} for Al^{3+} in the Y site is considerably smaller (about half) than that of Fe-rich pumpellyite. On the other hand, some edges of YO_6-octahedra along the b axis are shared with WO_7-polyhedra, and the effect of the ionic substitution in the Y site on the b axis is thus smaller than that on the a axis. Perhaps due to this, the Δb per Cr^{3+} (apfu) of 0.015 Å is almost identical with the Δb per Fe^{3+} (apfu) of 0.016 Å.

TABLE 9. Angular and bond-length distortions of the X and Y octahedral sites

Sample	X site			Y site			Reference
	$\sigma_\theta(oct)^2$†	$<l_{oct}>$†	$DI(oct)$†	$\sigma_\theta(oct)^2$†	$<l_{oct}>$†	$DI(oct)$†	
ocp1211	16.25	1.006	0.027	35.22	1.0112	0.022	This study
ocp0604	18.12	1.007	0.027	37.22	1.0117	0.020	This study
ocp1028	17.10	1.007	0.028	36.94	1.0115	0.020	This study
ocp1013	17.02	1.007	0.028	34.41	1.0106	0.017	This study
ocp1016	14.91	1.006	0.028	35.60	1.0111	0.019	This study
Sarani chromian pumpellyite	13.56	1.005	0.019	37.69	1.012	0.021	Nagashima and Akasaka (2007)
MTS	14.41	1.007	0.034	36.39	1.0115	0.021	Nagashima et al. (2006b)
KGH	18.41	1.008	0.035	35.25	1.0114	0.022	Nagashima et al. (2007b)
HR*	21.08	1.008	0.030	31.63	1.011	0.026	Galli and Arberti (1969)
Julgoldite	14.55	1.006	0.029	29.59	1.009	0.014	Allmann and Donnay (1973)
Pumpellyite	16.83	1.007	0.028	37.46	1.012	0.022	Yoshiasa and Matsumoto (1985)
HR*	18.20	1.006	0.011	28.39	1.009	0.018	Artioli and Geiger (1994)
K1*	26.64	1.010	0.030	34.01	1.01	0.022	Artioli and Geiger (1994)
BU*	19.79	1.008	0.027	30.16	1.009	0.019	Artioli and Geiger (1994)
Bombay julgoldite–(Fe³⁺)	5.98	1.002	0.018	16.30	1.005	0.012	Artioli et al. (2003)
Poppiite	18.74	1.007	0.027	29.40	1.009	0.019	Brigatti et al. (2006)

* Sample lavels of Galli and Alberti (1969) and Artioli and Geiger (1994).
† $<l_{oct}> = \Sigma(l_i - l_o)^2/6$ (l_i = each bond length, l_o = center-to-vertex distance for and octahedron with Oh symmetry, whose volume is equal to that of a distorted octahedra with bond length l_i) (Robinson et al. 1971), $\Delta l_{oct} = 1/6\Sigma|R_i - R_{avg}|/R_{avg}$ (R_i = each bond length; R_{avg} = average distance for an octahedron) (Baur 1974), and $\sigma_\theta(oct)^2 = \Sigma(\theta_i - 90°)^2/11$ (θ_i = O-M-O angle) (Robinson et al. 1971).

Site distortion

Site distortion is also a good indicator of structural changes caused by ionic substitutions. The bond-length distortion parameter $<\lambda_{oct}>$ defined by Robinson et al. (1971), $DI(oct)$ (Baur 1974), and the angular distortion parameter $\sigma_\theta(oct)^2$ (Robinson et al. 1971) are listed in Table 9. As pointed out by Artioli and Geiger (1994), the $\sigma_\theta(oct)^2_X$-$\sigma_\theta(oct)^2_Y$ and $<\lambda_{oct}>_X$-$<\lambda_{oct}>_Y$ diagrams reveal larger angular and bond-length distortions of the Y site than those of the X site. However, Nagashima et al. (2006) found that the distortion of the Y sites is smaller than the X site in terms of the distortion index $DI(oct)$ of Baur (1974). As shown in Table 9, the $DI(oct)$ values of the YO_6-octahedra for Osayama chromian pumpellyite are also lower than those of the XO_6-octahedra, although the Y site is more distorted than the X site in the distortion indices of Robinson et al. (1971). Thus, evaluation of site distortions of the XO_6- and YO_6-octahedra is critical, and both indices should be presented to show the degree of distortion for the X and Y sites. However, the $DI(oct)$ of the Y site for Osayama and Sarani chromian pumpellyite shows inverse relation with the mean ionic radius, as well as the results for Fe-rich pumpellyite (Nagashima et al. 2006), indicating change of the YO_6-octahedra to more regular form with the substitution of Cr^{3+} for Al^{3+}. It also illustrates the usefulness of Baur's distortion index for representation of octahedral site distortion in pumpellyite.

REFERENCES CITED

Akasaka, M., Kimura, Y., Omori, Y., Sakakibara, M., Shinno, I., and Togari, K. (1997) ⁵⁷Fe Mössbauer study of pumpellyite-okhotskite-julgoldite series minerals. Mineralogy and Petrology, 61, 181–198.
Allmann, R. and Donnay, G. (1973) The crystal structure of julgoldite. Mineralogical Magazine, 39, 271–281.
Artioli, G. and Geiger, C.A. (1994) The crystal chemistry of pumpellyite: An X-ray Rietveld refinement and ⁵⁷Fe Mössbauer study. Physics and Chemistry of Minerals, 20, 443–453.

Artioli, G., Pavese, A., Belotto, M., Collins, S.P., and Luchetti, G. (1996) Mn crystal chemistry in pumpellyite: A resonant scattering powder diffraction Rietveld study using synchrotron radiation. American Mineralogist, 81, 603–610.
Artioli, G., Geiger, C.A., and Dapiaggi, M. (2003) The crystal chemistry of julgoldite-Fe³⁺ from Bombay, India, studied using synchrotron X-ray powder diffraction and ⁵⁷Fe Mössbauer spectroscopy. American Mineralogist, 88, 1084–1090.
Baur, W.H. (1974) The geometry of polyhedral distortions. Predictive relationships for the phosphate group. Acta Crystallographica, B30, 1195–1215.
Brese, N.E. and O'Keeffe, M. (1991) Bond-valence parameters for solids. Acta Crystallographica, B47, 192–197.
Brigatti, M.F., Caprilli, E., and Marchensini, M. (2006) Poppiite, the V³⁺ end-member of the pumpellyite group: Description and crystal structure. American Mineralogist, 91, 584–588.
Brown, I.D. and Altermatt, D. (1985) Bond-valence parameters obtained from a systematic analysis of the Inorganic Crystal Structure Database. Acta Crystallographica, A29, 266–282.
Creagh, D.C. and Hubbell, J.H. (1992) X-ray absorption (or attenuation) coefficients. In A.J.C. Wilson, Ed., International Tables for Crystallography, vol. C, p. 200–206. Kluwer Academic Publishers, Boston.
Creagh, D.C. and McAuley, W.J. (1992) X-ray dispersions corrections. In A.J.C. Wilson, Ed., International Tables for Crystallography, vol. C, p. 206–222. Kluwer Academic Publishers, Boston.
Cromer, D.T. and Waber, J.T. (1974) In A.J.C. Wilson, Ed., International Tables for X-ray Crystallography, vol. IV, p. 200–206. The Kynoch Press, Birmingham, U.K.
Farmer, V.C. (1974) The Infrared Spectra of Minerals. Mineralogical Society Monograph.
Franks, F. (1973) Water: A comprehensive treatise, vol. 2, 684 p. Plenum, New York.
Galli, E. and Alberti, A. (1969) On the crystal structure of pumpellyite. Acta Crystallographica, B25, 2276–2281.
Hamada, M., Seto, S., Akasaka, M., and Takasu, A. (2008) Chromian pumpellyite and associated chromian minerals from Sangun metamorphic rocks, Osayama, southwest Japan. Journal of Mineralogical and Petrological Sciences, 103, 390–399.
Hatert, F., Pasero, M., Perchiazzi, N., and Theye, T. (2007) Pumpellyite-(Al), a new mineral from Betrix, Belgian Ardennes. European Journal of Mineralogy, 19, 247–253.
Hawthorne, F.C., Ungaretti, L., and Oberti, R. (1995) Site populations in minerals: Terminology and presentation of results of crystal-structure refinement. Canadian Mineralogist, 33, 907–911.
Higashi, T. (1995) Abscor-Empirical correction based on Fourier series approximation. Rigaku Corporation, Tokyo, Japan.
Ivanov, O.K., Arkhangel'skaya, V.A., Miroshnikova, L.O., and Shilova, T.A. (1981) Shuiskite, the chromium analogue of pumpellyite, from the Bisersk deposit, Urals. Zapiski Vsesojuznogo Mineralogiceskogo Obscestva, 110, 508–512.
Momma, K. and Izumi, F. (2008) VESTA: A three dimensional visualization system for electronic and structural analysis. Journal of Applied Crystallography, 41, 653–658.
Moore, P.B. (1971) Julgoldite, the Fe²⁺-Fe³⁺ dominant pumpellyite. Lithos, 4, 93–99.
Nagashima, M. (2006) Distribution of transition elements among octahedral sites

in epidotes, pumpellyites and related minerals and the effect on their crystal structure. Unpublished Ph.D. thesis, Shimane University, Japan.

Nagashima, M. and Akasaka, M. (2007) The distribution of chromium in chromian pumpellyite from Sarani, Urals, Russia: A TOF neutron and X-ray Rietveld study. Canadian Mineralogist, 45, 837–846.

Nagashima, M., Ishida, T., and Akasaka, M. (2006) Distribution of Fe among octahedral sites and its effect on the crystal structure of pumpellyite. Physics and Chemistry of Minerals, 33, 178–191.

Nakano, S., Makino, K., and Eriguchi, T. (2001) Microtexture and water content of alkali feldspar by Fourier-transform infrared microspectroscopy. Mineralogical Magazine, 65, 675–683.

Palache, C. and Vassar, H.E. (1925) Some minerals of the Keweenawan copper deposits: Pumpellyite a new mineral; sericite; saponite. American Mineralogist, 10, 412–418.

Passaglia, E. and Gottardi, G. (1973) Crystal chemistry and nomenclature of pumpellyites and julgoldites. Canadian Mineralogist, 12, 219–223.

Robinson, K., Gibbs, G.V., and Ribbe, P.H. (1971) Quadratic elongation: A quantitative measure of distortion in coordination polyhedra. Science, 172, 567–570.

Sakamoto, S. (1997) Chemical composition of kosmochlor and related minerals from tectonic blocks within the Osayama ultramafic body in the Sangun metamorphic belt, Southwest Japan. Memoir of the Faculty of Science and Engineering of Shimane University, Series A, 31, 217–241.

Shannon, R.D. (1976) Revised effective ionic radii and systematic studies of interatomic distances in halides and chalcogenides. Acta Crystallographica, A32, 751–767.

Sheldrick, G.M. (1997) SHELXL-97. A program for crystal structure refinement. University of Göttingen, Germany.

Togari, K. and Akasaka, M. (1987) Okhotskite, a new mineral, an Mn^{3+}-dominant member of the pumpellyite group, from the Kokuriki mine, Hokkaido, Japan. Mineralogical Magazine, 51, 611–614.

Yoshiasa, A. and Matsumoto, T. (1985) Crystal structure refinement and crystal chemistry of pumpellyite. American Mineralogist, 70, 1011–1019.